

Strong XUV irradiation of the Earth-sized exoplanets orbiting the ultracool dwarf TRAPPIST-1

Peter J. Wheatley,^{1*} Tom Louden,¹ Vincent Bourrier,² David Ehrenreich²
and Michaël Gillon³

¹*Dept. of Physics, University of Warwick, Gibbet Hill Road, Coventry CV4 7AL, UK*

²*Observatoire de l'Université de Genève, 51 chemin des Maillettes, 1290 Versoix, Switzerland*

³*Institut d'Astrophysique et de Géophysique, Université de Liège, Allée du 6 Août 19C, 4000 Liège, Belgium*

Accepted XXX. Received YYY; in original form ZZZ

ABSTRACT

We present an *XMM-Newton* X-ray observation of TRAPPIST-1, which is an ultracool dwarf star recently discovered to host three transiting and temperate Earth-sized planets. We find the star is a relatively strong and variable coronal X-ray source with an X-ray luminosity similar to that of the quiet Sun, despite its much lower bolometric luminosity. We find $L_X/L_{\text{bol}} = 2 - 4 \times 10^{-4}$, with the total XUV emission in the range $L_{\text{XUV}}/L_{\text{bol}} = 6 - 9 \times 10^{-4}$. Using a simple energy-limited model we show that the relatively close-in Earth-sized planets, which span the classical habitable zone of the star, are subject to sufficient X-ray and EUV irradiation to significantly alter their primary and perhaps secondary atmospheres. Understanding whether this high-energy irradiation makes the planets more or less habitable is a complex question, but our measured fluxes will be an important input to the necessary models of atmospheric evolution.

Key words:

1 INTRODUCTION

Gillon et al. (2016) announced the discovery of a remarkable system of three Earth-sized planets orbiting a nearby ultracool dwarf star of spectral type M8, TRAPPIST-1. The planets are transiting, providing precise radii, and because the host star is small and cool the transits are deep and the planets are temperate despite their relatively short orbital periods.

The three planets are most likely all outside the classical habitable zone, two closer-in and one beyond (although the outer planet has an uncertain orbit that could place it in the habitable zone). Nevertheless, the factors that influence habitability are complex and uncertain and Gillon et al. (2016) point out that habitable conditions might exist at the terminators of the inner planets that are presumably tidally-locked, while tidal heating of the outer planet might render it habitable as well. Either way, the small size and low temperature of the star, and the proximity of the system to Earth (12 pc), provide by far the best opportunity to date to study the atmospheres of cool, Earth-sized exoplanets.

An important factor influencing the evolution of planetary atmospheres and their habitability is the X-ray and

extreme-ultraviolet (EUV) radiation emitted by their parent stars (together often termed XUV radiation). Mass loss from exoplanetary atmospheres is observed directly in ultraviolet transit observations of giant planets (e.g. Vidal-Madjar et al. 2003; Lecavelier des Etangs et al. 2012; Ehrenreich et al. 2015) and this is thought to be the result of XUV irradiation heating of the planetary exosphere and driving hydrodynamic escape (Lammer et al. 2003). The long term effects of XUV irradiation on the habitability of terrestrial planets are complex and uncertain, and while some planets might be rendered uninhabitable through atmospheric stripping, others may become habitable through the removal of a massive primary atmosphere of H/He (e.g. Owen & Mohanty 2016). Water might be removed from some habitable zone planets by photolysis and H evaporation (e.g. Bolmont et al. 2016), perhaps leading to abiotic oxygen-dominated atmospheres (Wordsworth & Pierrehumbert 2014), while in other planets the evaporation might prevent the atmosphere of an outgassing planet from becoming too dense. It has also been suggested that XUV irradiation might expand a secondary atmosphere beyond the magnetosphere of the planet, where it becomes vulnerable to erosion by the stellar wind (e.g. Lammer et al. 2011).

Ultracool dwarfs are known to exhibit stellar activity, but the activity level seems to decrease steeply to later spec-

* E-mail: P.J.Wheatley@warwick.ac.uk

tral types, with L_X/L_{bol} values dropping by at least two orders of magnitude from saturated emission of 10^{-3} for mid-M stars (e.g. Pizzolato et al. 2003; Wright et al. 2011) to $< 10^{-5}$ for mid-L dwarfs (e.g. Berger et al. 2010). Williams et al. (2014) confirm the breakdown of saturated X-ray emission for spectral types later than M6, but find that a population of objects later than M7 with X-ray emission characteristic of mid-M stars is not excluded.

TRAPPIST-1 has been found to exhibit chromospheric $H\alpha$ emission at a level of $L_{H\alpha}/L_{\text{bol}} = 2.5 \times 10^{-4}$, which is found to be typical for its M8 spectral type and weaker than seen in mid-M stars (Reiners & Basri 2010). TRAPPIST-1 also has a relative weak magnetic field strength of ~ 600 G (also Reiners & Basri 2010), which is lower than mid-M stars with the same short spin period of 1.40 ± 0.05 d. It may therefore be expected to have X-ray emission considerably weaker than mid-M stars, and indeed Bolmont et al. (2016) assumed $L_X/L_{\text{bol}} < 10^{-5}$ in a recent study of water loss from the Earth-sized planets of TRAPPIST-1.

In this letter we present an *XMM-Newton* observation of TRAPPIST-1 that allows us to measure the X-ray luminosity of the star, estimate its EUV luminosity, and hence consider the effects of XUV irradiation on the Earth-sized exoplanets.

2 OBSERVATIONS

The host star of the TRAPPIST-1 system (=2MASS J23062928–0502285) was observed with *XMM-Newton* for 30 ks on 17th December 2014 (ObsID: 0743900401; PI: Stelzer) using the thin optical blocking filters. An X-ray source is clearly detected at the proper-motion corrected 2MASS position of the ultracool dwarf (Cutri et al. 2003; Costa et al. 2006). The source is soft, being visible in pipeline processed EPIC-pn images in the 0.2–0.5 and 0.5–1.0 keV bands, but not in the higher energy bands. The *XMM-Newton* pipeline source detection also identifies a source at this position, with an offset of 3.1 arcsec from the expected source position. This offset is consistent with the known accuracy of the *XMM-Newton* astrometric frame (Watson et al. 2009) and we find the offset drops to 1.27 arcsec when the *XMM-Newton* astrometry is rectified against the USNO B1.0 catalogue.

We extracted X-ray lightcurves and spectra for TRAPPIST-1 from the EPIC-pn camera using the pipeline source detect position and a 20 arcsec radius aperture. The EPIC-pn camera observed for 28.0 ks and had an effective exposure time of 24.9 ks. For such a soft source only a small proportion of the X-ray events are detected in the EPIC-MOS cameras so we limited our analysis to the EPIC-pn. The background counts were estimated using a source-free circular region of radius 51.5 arcsec located at the same end of the same CCD. We followed the standard data reduction methods as described in data analysis threads provided with the Science Analysis System¹ (SAS version 14.0). The spectrum was binned to a minimum of 10 counts per bin, with the additional requirement that the EPIC-pn spectral resolution would not be oversampled by more than a factor of 3.

We fitted the spectrum using XSPEC² (version 12.8). Our fitted parameters were determined using the Cash statistic (Cash 1979) and our quoted errors correspond to 68% confidence intervals.

A number of background flares occurred during the observation, however we did not filter these time intervals when creating the data products presented here (as suggested in the SAS threads) because we wanted to inspect the entire X-ray light curve and measure X-ray fluxes averaged across the observation (see Sect. 3).

3 RESULTS

3.1 X-ray light curve

Figure 1 shows the *XMM-Newton* X-ray light curve of TRAPPIST-1. The background light curve (red points in the top panel) shows that background flares occurred during the observation, accounting for much of the variability in the raw source light curve (green points in top panel), but the source remains variable after the background has been subtracted (middle panel of Fig. 1). It can be seen that the star was brighter at the beginning and the end of the observation. This variability is statistically significant, with a χ^2 of 85.6 for 27 degrees of freedom when compared to the weighted mean of all the data points. The 7.8 hr observation covers 23% of the 1.40 d spin period of the star (Gillon et al. 2016) so it is likely that at least some of this variability is due to rotational modulation.

In the bottom panel of Fig. 1 we plot a measure of the hardness of the X-ray spectrum of TRAPPIST-1 during the beginning, middle and end of the observation. Hardness ratios are a simple method with which to identify variations in the X-ray spectrum, and in this case we have calculated the ratio of the X-ray count rate in the 0.5–1.5 keV band to the count rate in the 0.15–0.5 keV band. To the precision of the current dataset, it can be seen that the hardness ratio is consistent with the X-ray spectrum remaining constant throughout the observation, despite the flux variations apparent in the light curve. There is a hint that the hardness may have increased during the brightening at the end of the observation, and an increase in hardness would be expected if this brightening were due to flaring activity.

3.2 Spectral analysis

The *XMM-Newton* EPIC-pn spectrum of TRAPPIST-1 is plotted in Fig. 2. The X-ray spectrum is very soft and shows evidence of line emission between 0.5 and 1.0 keV. These features are characteristic of coronal emission from late type stars. We fitted the spectrum using the APEC model for a collisionally-ionised optically-thin plasma (Smith et al. 2001), finding a poor fit with a single temperature model, but a good fit with a two temperature model (χ^2 of 11.9 with 17 degrees of freedom). The model and residuals to this fit are plotted in the top and middle panels of Fig. 2 respectively. The fitted temperatures are $kT = 0.15^{+0.02}_{-0.01}$ and $0.83^{+0.16}_{-0.10}$ keV. In reality, coronal X-ray emission is expected to be the sum of emission from a wide and continuous range

¹ <http://www.cosmos.esa.int/web/xmm-newton/sas>

² <https://heasarc.gsfc.nasa.gov/xanadu/xspec/>

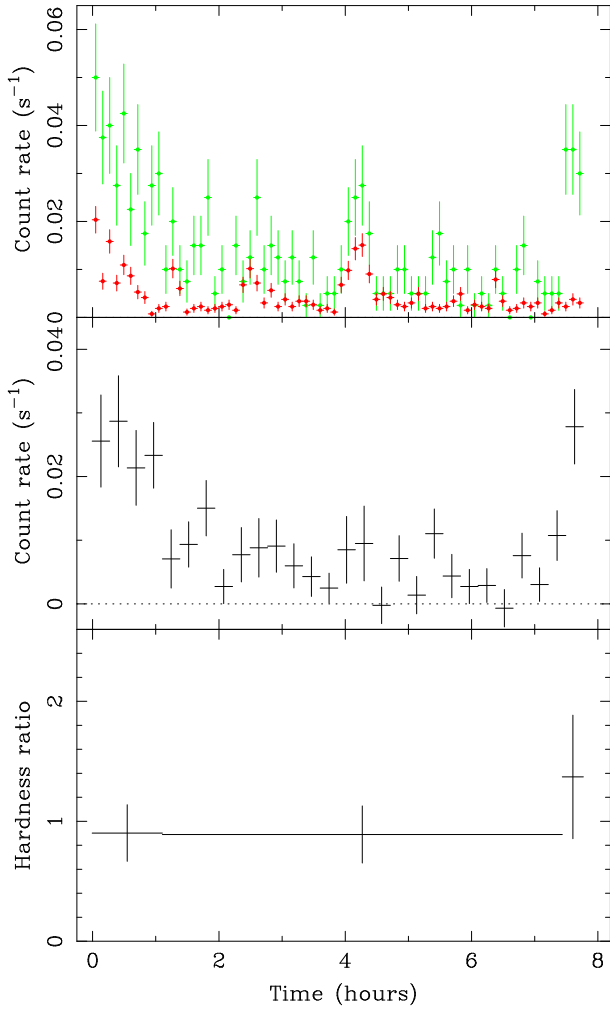


Figure 1. Top: the raw source (green) and scaled background (red) X-ray light curve of TRAPPIST-1 in the 0.15–1.5 keV band with the *XMM-Newton* EPIC-pn camera. The data are plotted in 400 s bins. Middle: the background-subtracted X-ray light curve of TRAPPIST-1 in 1000 s bins. Bottom: the hardness of the source calculated as the ratio of X-ray counts in the 0.5–1.5 keV and 0.15–0.5 keV bands.

of temperatures (e.g. Louden et al. 2016), but at low spectral resolution and with modest signal-to-noise ratios a two temperature model usually provides an adequate approximation (e.g. Pillitteri et al. 2014).

As expected for such a nearby X-ray source (12.1 ± 0.4 pc; Costa et al. 2006) we found that the interstellar X-ray absorption is too low to be constrained usefully by the X-ray spectrum. Consequently we chose to fix the interstellar absorption in our models at a value of $N_{\text{H}} = 3.7 \times 10^{18} \text{ cm}^{-2}$ based on an assumed local interstellar neutral hydrogen density of 0.10 cm^{-3} (Redfield & Linsky 2000). We modeled the absorption with the *tbabs* model in XSPEC (Wilms et al. 2000), and found that it had a negligible effect on our fitted temperatures and X-ray fluxes.

Elemental abundances are also poorly constrained by the X-ray spectrum and we left them fixed at Solar values (Asplund et al. 2009).

Our fitted X-ray energy fluxes for TRAPPIST-1 are presented in Table 1, together with X-ray luminosities cal-

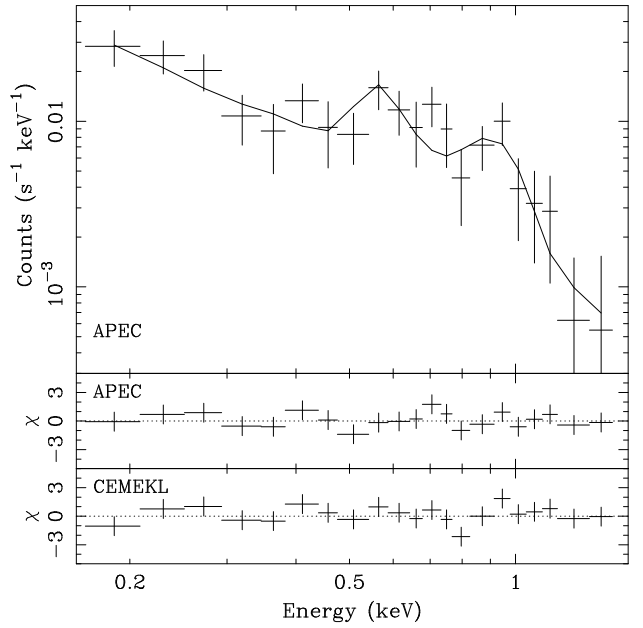


Figure 2. The *XMM-Newton* EPIC-pn spectrum of TRAPPIST-1 fitted with our two temperature APEC model (top). The middle panel shows the normalised residuals to this fit, while the bottom panel shows the residuals to our fit with the CEMEKL model.

Table 1. Fitted X-ray fluxes and luminosities for TRAPPIST-1 in different energy bands. APEC refers to our two temperature model. CEMEKL is our multi-temperature model where the emission measure distribution is defined by a power law.

Energy range (keV)	X-ray flux ^a		Luminosity ^b	
	APEC	CEMEKL	APEC	CEMEKL
0.100 – 2.40	2.16 ± 0.18 0.21	4.49 ± 0.44 0.70	3.79 ± 0.36 0.31	7.89 ± 0.86 1.28
0.124 – 2.48	2.06 ± 0.15 0.18	2.94 ± 0.19 0.36	3.62 ± 0.36 0.31	5.16 ± 0.68 0.41
0.150 – 2.40	1.98 ± 0.13 0.19	2.42 ± 0.13 0.31	3.48 ± 0.28 0.37	4.25 ± 0.30 0.58
0.200 – 2.40	1.83 ± 0.11 0.16	1.88 ± 0.09 0.22	3.21 ± 0.24 0.32	3.30 ± 0.22 0.42

^a $\times 10^{-14} \text{ erg s}^{-1} \text{ cm}^{-2}$

^b $\times 10^{26} \text{ erg s}^{-1}$

culated from the known distance to the star (12.1 ± 0.4 pc; Costa et al. 2006). We have given values for a range of energy intervals in order to facilitate comparison with other studies of the coronal X-ray emission of late type stars.

In order to calculate our X-ray fluxes in the commonly-used *ROSAT* PSPC band (0.1–2.4 keV) it was necessary to extrapolate our fitted model beyond the soft cut-off of our EPIC-pn X-ray spectrum at 0.166 keV. This extrapolation is sensitive to the number and distribution of temperature components employed in the model, and it is possible that our simple two temperature model under-predicts the X-ray flux in the 0.1–2.4 keV band. In order to investigate the uncertainty in this extrapolation we also fitted our spectrum with the CEMEKL model in XSPEC, which calculates the X-ray spectrum of an optical-thin plasma with a continuous range of temperatures up to a maximum and with the emission measure distribution defined by a power law (e.g. Done & Osborne 1997; Baskill et al. 2005). We used the version of CEMEKL based on the same APEC model employed in our two temperature fit. We find an almost

equally good fit to the spectrum with this model (χ^2 of 15.7 with 19 degrees of freedom) and the residuals are plotted in the lower panel of Fig. 2. In this fit the emission measure rises steeply to lower temperatures, with a power law index of -0.81 ± 0.15 . The maximum temperature is poorly constrained to $kT_{\max} > 1.23$ keV and we left this parameter fixed to $kT_{\max} = 5$ keV while evaluating the X-ray fluxes.

The fluxes and corresponding luminosities for the CEMEKL fit are also presented in Table 1, and it can be seen that the fluxes of the two-temperature APEC model and the CEMEKL model are consistent within the energy band covered by the EPIC-pn spectrum, but diverge as the model is extrapolated down to 0.1 keV. This is as expected because the two temperature model does not account for the emission from cooler plasma that may contribute significantly below the EPIC-pn band, while the power law model for the distribution of emission measures may be too steep below the EPIC-pn band and over-predict the contribution from lower temperatures. In Sect. 4 we assume that the true 0.1–2.4 keV X-ray luminosity falls between the best fitting values from these model extremes, i.e. in the range $(3.8\text{--}7.9)\times 10^{26}$ erg s $^{-1}$.

4 DISCUSSION

Our spectral analysis in Sect. 3.2 and X-ray luminosities in Table 1 show that TRAPPIST-1 is a relatively strong coronal X-ray source. It has the same 0.1–2.4 keV X-ray luminosity as the quiet Sun (6×10^{26} erg s $^{-1}$, Judge et al. 2003) despite its photospheric luminosity of only $0.000525 \pm 0.000036 L_{\odot}$ (Filippazzo et al. 2015).

The L_x/L_{bol} ratio of the star is in the range $(2\text{--}4)\times 10^{-4}$, which places it below the canonical value of 10^{-3} for saturated X-ray emission of stars with spectral types G to mid-M (e.g. Pizzolato et al. 2003; Wright et al. 2011). TRAPPIST-1 is a reasonably rapidly rotating star, with a spin period of 1.40 ± 0.05 d, and so it might be expected to exhibit saturated X-ray emission for its spectral type. The relatively low flux compared to the canonical saturated value might then reflect the known decrease in stellar activity to spectral types later than M6 (e.g. Berger et al. 2010; Williams et al. 2014). However, inspection of the distribution of L_x/L_{bol} values for individual earlier-type saturated stars in Wright et al. (2011) shows a considerable spread around the mean value of 7×10^{-4} , and many earlier type stars have L_x/L_{bol} in the range $(2\text{--}4)\times 10^{-4}$ that we observe for TRAPPIST-1. Consequently, the X-ray emission of TRAPPIST-1 can also be considered to be consistent with the saturated emission of earlier type M stars.

In order to consider the possible effects of X-ray and EUV irradiation on the atmospheres and possible oceans of the Earth-sized planets orbiting TRAPPIST-1 we estimate energy-limited mass loss rates (e.g. Lammer et al. 2003; Lecavelier Des Etangs 2007; Louden et al. 2016) as

$$\dot{M} = \frac{\eta\pi F_{XUV}\alpha^2 R_p^3}{GM_p K} = \frac{\eta I_{XUV}\alpha^2 R_p}{GM_p K} \quad (1)$$

where F_{XUV} is the combined X-ray and EUV fluxes incident on the planet, I_{XUV} is the total X-ray and EUV irradiation of the planet, G is the gravitational constant and M_p and R_p are the mass and radius of the planet respectively. The factor K accounts for the reduced energy required to escape

the Roche lobe of the planet (Erkaev et al. 2007). We set the quantity α to unity, which is designed to take account of the increased cross-sectional area of planets to EUV radiation. This is an important correction for hot gaseous planets, but probably negligible for cooler terrestrial planets.

In order to calculate energy-limited escape rates we need to estimate the EUV flux of the star, which is not covered by the *XMM-Newton* bandpass. To do this we employ the scaling relation of Chadney et al. (2015), which is an empirical relationship between the X-ray flux at the surface of the star and the relative strength of the X-ray and EUV emission. We cannot be sure that this relation applies to such a late spectral type as TRAPPIST-1, but we are encouraged that the Chadney et al. (2015) study includes a mid-M star, and that our measured surface X-ray flux for TRAPPIST-1 ($4.6\text{--}9.5\times 10^5$ mW m $^{-2}$) lies in the middle of the range calibrated by the empirical relation. Using this relation we find $F_{EUV}/F_X = 1.78$ for the surface flux calculated from our APEC spectral fit (Table 1) and $F_{EUV}/F_X = 1.31$ for our CEMEKL model.

In Table 2 we present our calculated values for F_X , F_{EUV} and I_{XUV} , as well as energy-limited mass loss rates for each planet assuming an energetic efficiency of $\eta = 0.1$. We give values only for the APEC model since the CEMEKL values are simply all a factor of 1.7 higher. It can be seen that these escape rates could be highly significant for Earth-like planets with atmospheric masses of around 5×10^{21} g and ocean masses of around 1×10^{24} g. On the timescale of a Gyr, all three planets could have been stripped of atmospheres and oceans. Even at the wider possible separations, TRAPPIST-1d could be very substantially eroded, including for instance the entire H component of the UV photo-dissociated water content of the Earth.

On the other hand, energy-limited mass loss is rather simplistic and can only provide an upper limit to mass loss rates, neglecting as it does the radiation physics and hydrodynamics of the planetary atmosphere and its composition. Owen & Mohanty (2016) for instance show that energy limited mass loss models can considerably over-estimate escape rates. They also show that rather strong XUV irradiation is actually required for a terrestrial planet to become habitable if it is formed with a substantial H/He primary atmosphere.

Bolmont et al. (2016) have carried out an investigation of the likely rates of water loss from Earth-sized exoplanets in the habitable zones of ultracool dwarfs, and in TRAPPIST-1 in particular. They conclude that TRAPPIST-1b and -1c are likely to be completely desiccated by XUV irradiation, but that TRAPPIST-1d may have held onto most of its initial water content. However, these authors assume $L_{XUV}/L_{bol} < 10^{-5}$ for TRAPPIST-1, which is at least fifty times smaller than the value we measure here. On the face of it this seems to make a significant water content on TRAPPIST-1d also unlikely, although Bolmont et al. (2016) do list a number of mechanisms that influence water loss and require further investigation. Water might, for instance, survive in cold traps on the night sides or at the poles of highly-irradiated tidally-locked planets (e.g. Leconte et al. 2013; Menou 2013).

The TRAPPIST-1 system presents a fabulous opportunity to study the atmospheres of Earth-sized planets as well as the complex and uncertain mechanisms controlling planet habitability. Whatever the mechanisms at play, the

Table 2. The X-ray and EUV irradiation of the individual Earth-sized planets in the TRAPPIST-1 system. The symbols F_X and F_{EUV} denote the energy fluxes at the planet, while I_{XUV} is the total X-ray and EUV energy input to each planet. Mass loss rates were calculated assuming energy-limited atmospheric escape with an efficiency of 10%. The figures here are based on our best-fitting APEC fluxes of Table 1 and it should be noted that our CEMEKL fits suggest that all of these figures could be higher by a factor 1.7. Orbital separations and planet radii are from Gillon et al. (2016).

Planet name	Separation (AU)	Radius (R_{Earth})	F_X ($erg\ s^{-1}\ cm^{-2}$)	F_{EUV} ($erg\ s^{-1}\ cm^{-2}$)	I_{XUV} ($\times 10^{20}\ erg\ s^{-1}$)	($\times 10^7\ g/s$)	Mass loss (Earth oceans ^c /Gyr)
TRAPPIST-1b	0.01111	1.113	1092.	1950.	48.1	118.	29.
TRAPPIST-1c	0.01522	1.049	582.	1039.	22.7	47.2	12.
TRAPPIST-1d	0.022 ^a	1.168	278.	497.	13.5	29.6	7.2
TRAPPIST-1d	0.058 ^b	1.168	40.1	71.6	1.94	3.85	0.93
TRAPPIST-1d	0.146 ^a	1.168	6.32	11.3	0.306	0.587	0.14

^a The minimum and maximum possible orbital separations for TRAPPIST-1d.

^b The most likely orbital separation for TRAPPIST-1d.

^c Taken to be $1.3 \times 10^{24}\ g$.

X-ray and XUV fluxes determined here will be a vital input to such studies.

5 CONCLUSIONS

We have analysed data from an *XMM-Newton* observation of TRAPPIST-1, which is the ultracool host star of a system of three transiting Earth-sized planets. We find that the star is a relatively strong and variable X-ray source, with a similar luminosity to that of the quiet Sun despite its much lower bolometric luminosity. We show that the relatively close-in Earth-sized planets, which span the classical habitable zone of the star, are subject to sufficient X-ray and EUV irradiation to significantly alter their primary and perhaps secondary atmospheres. Whether this high-energy irradiation acts to make the exoplanets more or less habitable is uncertain, but our XUV fluxes will be important inputs to models attempting to unravel the evolution of this fascinating system.

ACKNOWLEDGEMENTS

P.W. is supported by STFC consolidated grant (ST/L000733/1). T.L. is supported by a STFC studentship.

REFERENCES

Asplund M., Grevesse N., Sauval A. J., Scott P., 2009, *ARA&A*, **47**, 481
 Baskill D. S., Wheatley P. J., Osborne J. P., 2005, *MNRAS*, **357**, 626
 Berger E., et al., 2010, *ApJ*, **709**, 332
 Bolmont E., et al., 2016, *MNRAS*, submitted
 Cash W., 1979, *ApJ*, **228**, 939
 Chadney J. M., Galand M., Unruh Y. C., Koskinen T. T., Sanz-Forcada J., 2015, *Icarus*, **250**, 357
 Costa E., Méndez R. A., Jao W.-C., Henry T. J., Subasavage J. P., Ianna P. A., 2006, *AJ*, **132**, 1234
 Cutri R. M., et al., 2003, VizieR Online Data Catalog, **2246**
 Done C., Osborne J. P., 1997, *MNRAS*, **288**, 649
 Ehrenreich D., et al., 2015, *Nature*, **522**, 459
 Erkaev N. V., Kulikov Y. N., Lammer H., Selsis F., Langmayr D., Jaritz G. F., Biernat H. K., 2007, *A&A*, **472**, 329
 Filippazzo J. C., Rice E. L., Faherty J., Cruz K. L., Van Gordon M. M.,Looper D. L., 2015, *ApJ*, **810**, 158

Gillon M., et al., 2016, *Nature*, in press
 Judge P. G., Solomon S. C., Ayres T. R., 2003, *ApJ*, **593**, 534
 Lammer H., Selsis F., Ribas I., Guinan E. F., Bauer S. J., Weiss W. W., 2003, *ApJ*, **598**, L121
 Lammer H., Lichtenegger H. I. M., Khodachenko M. L., Kulikov Y. N., Griessmeier J., 2011, in Beaulieu J. P., Dieters S., Tinetti G., eds, *Astronomical Society of the Pacific Conference Series Vol. 450, Molecules in the Atmospheres of Extrasolar Planets*. p. 139
 Lecavelier Des Etangs A., 2007, *A&A*, **461**, 1185
 Lecavelier des Etangs A., et al., 2012, *A&A*, **543**, L4
 Lecointe J., Forget F., Charnay B., Wordsworth R., Selsis F., Millour E., Spiga A., 2013, *A&A*, **554**, A69
 Louden T., Wheatley P. J., Briggs K., 2016, *MNRAS*, in press
 Menou K., 2013, *ApJ*, **774**, 51
 Owen J. E., Mohanty S., 2016, *MNRAS*, p. stw959
 Pillitteri I., Wolk S. J., Lopez-Santiago J., Günther H. M., Sciortino S., Cohen O., Kashyap V., Drake J. J., 2014, *ApJ*, **785**, 145
 Pizzolato N., Maggio A., Micela G., Sciortino S., Ventura P., 2003, *A&A*, **397**, 147
 Redfield S., Linsky J. L., 2000, *ApJ*, **534**, 825
 Reiners A., Basri G., 2010, *ApJ*, **710**, 924
 Smith R. K., Brickhouse N. S., Liedahl D. A., Raymond J. C., 2001, *ApJ*, **556**, L91
 Vidal-Madjar A., Lecavelier des Etangs A., Désert J.-M., Ballester G. E., Ferlet R., Hébrard G., Mayor M., 2003, *Nature*, **422**, 143
 Watson M. G., et al., 2009, *A&A*, **493**, 339
 Williams P. K. G., Cook B. A., Berger E., 2014, *ApJ*, **785**, 9
 Wilms J., Allen A., McCray R., 2000, *ApJ*, **542**, 914
 Wordsworth R., Pierrehumbert R., 2014, *ApJ*, **785**, L20
 Wright N. J., Drake J. J., Mamajek E. E., Henry G. W., 2011, *ApJ*, **743**, 48

This paper has been typeset from a $\text{\TeX}/\text{\LaTeX}$ file prepared by the author.